Published in final edited form as:
Hepatology. 2013 October ; 58(4): 1326–1338. doi:10.1002/hep.26551.

Homeostatic generation of reactive oxygen species protects the zebrafish liver from steatosis

Justin M. Nussbaum[1], **Liuhong J. Liu**[1], **Syeda A. Hasan**[1], **Madeline Schaub**[1], **Allyson McClendon**[1], **Didier Y.R. Stainier**[2,3], and **Takuya F. Sakaguchi**[1,2,4]

[1]Department of Stem Cell Biology and Regenerative Medicine, Lerner Research Institute, Cleveland Clinic, Cleveland, Ohio 44195, USA

[2]Department of Biochemistry and Biophysics, Programs in Developmental and Stem Cell Biology, Genetics, and Human Genetics, and Liver Center, University of California, San Francisco, San Francisco, CA 94158

Abstract

Nonalcoholic fatty liver disease is the most common liver disease in both adults and children. The earliest stage of this disease is hepatic steatosis, in which triglycerides are deposited as cytoplasmic lipid droplets in hepatocytes. Through a forward genetic approach in zebrafish, we found that *guanosine monophosphate (GMP) synthetase* mutant larvae develop hepatic steatosis. We further demonstrate that activity of the small GTPase Rac1 and Rac1-mediated production of reactive oxygen species (ROS) are down-regulated in *GMP synthetase* mutant larvae. Inhibition of Rac1 activity or ROS production in wild-type larvae by small molecule inhibitors was sufficient to induce hepatic steatosis. More conclusively, treating larvae with hydrogen peroxide, a diffusible ROS that has been implicated as a signaling molecule, alleviated hepatic steatosis in both *GMP synthetase* mutant and Rac1 inhibitor-treated larvae, indicating that homeostatic production of ROS is required to prevent hepatic steatosis. We further found that ROS positively regulate the expression of the *triglyceride hydrolase* gene, which is responsible for the mobilization of stored triglycerides in hepatocytes. Consistently, inhibition of triglyceride hydrolase activity in wild-type larvae by a small molecule inhibitor was sufficient to induce hepatic steatosis. *Conclusion: de novo* GMP synthesis influences the activation of the small GTPase Rac1, which controls hepatic lipid dynamics through ROS-mediated regulation of *triglyceride hydrolase* expression in hepatocytes.

Introduction

The earliest stage of nonalcoholic fatty liver disease (NAFLD), hepatic steatosis, is characterized by excess accumulation of triglycerides (TG) in hepatocytes as lipid droplets(1). Hepatic steatosis is a risk factor for progression to nonalcoholic steatohepatitis (NASH), which can result in end-stage liver disease(1). There have been no successfully established treatments for NAFLD or NASH, leaving the reduction of known risk factors as the standard of treatment. Thus, understanding the molecular mechanisms that underlie each stage of NAFLD pathogenesis could lead to the development of therapeutic targets to lessen or reverse NAFLD progression. A previous genome-wide association study in humans estimated the heritability of NAFLD to be 26–27%(2). However, the number of human

[4]Author for correspondence: (sakagut2@ccf.org).
[3]Current address: Department of Developmental Genetics, Max Planck Institute for Heart and Lung Research, Bad Nauheim, Germany

genes known to associate with NAFLD is still limited(1), indicating the importance of finding new genes and pathways responsible for NAFLD pathogenesis.

In NAFLD pathogenesis, hepatic steatosis is induced by a net increase in the rate of TG acquisition and synthesis relative to export and oxidation. The removal of TGs from the liver is achieved by hydrolysis and subsequent β-oxidation of free fatty acids, or by secretion of lipoprotein particles containing TGs. Impairment of pathways regulating lipoprotein particle secretion can thus perturb the balance of TG homeostasis in the liver and lead to hepatic steatosis. Triglyceride hydrolase (TGH also known as Ces3 or Ces1d(3)) is an enzyme involved in the mobilization of stored TGs in hepatocytes to form lipoprotein particles(4–7).

In the progression of NAFLD from simple steatosis to NASH, it has been proposed that reactive oxygen species (ROS) play an important role(8). ROS are chemically reactive molecules containing oxygen, and common biological species include hydrogen peroxide (H_2O_2). ROS have been historically regarded as a toxic by-product of living cells that induce inflammatory responses and pathological conditions. Accumulating evidence now indicates, however, that ROS, especially the relatively stable H_2O_2 molecule, can function as intracellular second messengers at normal physiological levels(9, 10). The physiological role of ROS homeostasis in hepatocytes is, however, largely unknown.

In the cell, ROS can be generated in numerous biological reactions, primarily during mitochondrial metabolism and by ROS-generating enzymes, including the NOX family NADPH oxidases. The NADPH oxidases are multi-protein complexes that generate ROS(10). The roles of NADPH oxidases have been best characterized in phagocytes(10), however, this complex is found in many other tissues, including the liver. The regulatory subunit of Nox1 and Nox2 NADPH oxidases is the small GTPase Rac1(11), a member of the Rho GTPase family that regulates a wide variety of cellular functions. Rac1 works as a molecular switch by cycling between inactive and active states; when guanosine diphosphate (GDP) is bound, Rac1 is inactive, while Rac1 is activated by guanosine triphosphate (GTP) exchange. Therefore, GTP-bound Rac1 is necessary for the activation of Nox1 and Nox2 NAPDH oxidases.

GDP and GTP are generated from guanosine monophosphate (GMP) by transferring phosphate groups from ATP. In animal cells, GMP is synthesized through two distinct pathways: the *de novo* synthesis and salvage pathways(12). Since the salvage pathway is energetically more efficient, it is believed to be the primary supplier of guanine nucleotides. GTP is necessary for NOX2 NAPDH oxidase activation *in vitro*(13), but it is unclear how Rac1 and NADPH oxidase-mediated ROS generation is affected when guanosine nucleotides are reduced *in vivo*.

In this study, we implemented a forward genetic approach in zebrafish, which has proved to be a valuable strategy for identifying new genes and pathways that influence hepatic steatosis(14–18). We identified *GMP synthetase* mutant larvae as showing a hepatic steatosis phenotype, and subsequently found that they also show down-regulation of Rac1 activation and ROS generation. Accordingly, artificially reducing ROS levels through multiple mechanisms was sufficient to induce hepatic steatosis in wild-type zebrafish larvae, which were then subsequently rescued by artificially increasing ROS levels. These and other data suggest that physiological levels of ROS generation are required to protect the liver from accumulating excess hepatic lipid.

Materials and methods

Zebrafish husbandry and transgenic lines

Zebrafish (*Danio rerio*) larvae were obtained from crosses of wild-type AB/TL strain or heterozygous mutant fish and raised as previously described(19). The following transgenic and mutant lines were used: *GMP synthetase*^{s850}, *Tg(fabp10:GFP-CAAX)*^{lri1}, *and*, *Tg(fabp10:GFP*-DNRac1)^{lri4}.

Pharmacological treatments

The following molecules were used: Mycophenolic acid (Sigma Aldrich, Product #5255), Rac1 inhibitor (EMD Biosciences, Product #553502), diphenyleneiodonium chloride (DPI, Sigma Aldrich, Product #D2926), dimethyl p-nitrophenylphosphate (E600, Sigma Aldrich, Product #PS613) and N-acetyl-L-cystein (NAC, Sigma Aldrich, Product #A9165). All pharmacological treatments were administered with 1% dimethyl sulfoxide (DMSO) by volume. Concentrations of molecules used in this study are listed in supplementary table 2.

Oil Red O staining

Embryos were fixed at 7dpf and treated as previously described(17).

Rac1 activity assay

Rac1 Activity Assay Kit (Millipore) was used. Embryos were lysed and incubated with PAK-1 PBD-bound beads. After washing, beads were loaded on SDS-PAGE gels and blotted with anti-Rac1 (BD Transduction Laboratories, Cat. 610650) and β-tubulin (Abcam, Cat. 75123) antibodies.

Transmission electron microscopy

Electron microscopy was performed as previously described(19).

Nile Red staining, imaging and quantification

Embryos were fixed at 7dpf in 4% PFA overnight. Livers were removed and soaked in Nile Red (500ng/ml) along with TO-PRO3 Iodide nuclear stain for two hours at room temperature. Livers were then washed three times with PBS, mounted in Vectashield mounting media (Vector Laboratories) and imaged with a Leica SP5 confocal microscope (Leica Microsystems). Nile Red and GFP were simultaneously excited using a combination of 488 and 514 nm green argon lasers with emission of 505–520nm and 570–600nm, respectively. Images were then processed for 3-dimensional rendering using Imaris software (Bitplane Scientific).

The portion of hepatocytes containing lipid droplets was determined by blindly selecting a single z-plane from each confocal z-series and counting the number of cells that were positive or negative for the presence of lipid. Hepatocytes were identified by the expression of *Tg(fabp10:GFP-CAAX)*^{lri1}.

Immunohistochemistry and *in situ* hybridization

Immunohistochemistry and *in situ* hybridization were performed as previously described(19).

Real-time reverse transcriptase-PCR

Quantitative RT-PCR was performed as previously described(19) using the primers listed in supplementary table 1. The ΔΔCt method was used for relative quantification.

Triglyceride measurement

Triglycerides were measured in whole-body extracts of larvae. Total lipids were quantified using the Triglyceride (GPO) Liquid Reagent assay kit (Pointe Scientific). Lipid concentration (mg/ml) was normalized to protein concentration (mg/ml) using the BCA Protein Assay Kit (Pierce, Rockford, IL) according to the manufacturers instructions.

ROS measurement

Following pharmacological treatments, live larvae were incubated in 30μM 5-(and-6)-carboxy-2′,7′-dichlorodihydrofluorescein diacetate, acetyl ester (H2DCF) for 90 minutes and culture media was then measured for fluorescence at 485/535 nanometers on a BMG Labtech Fluorostar Optima Fluorescent Plate Reader (Life Technologies). Background fluorescence was subtracted by measuring fluorescence in identical conditions containing no larva.

Hydrolase activity assay

12–15 larvae were collected following pharmacological treatment and lysed by sonication in 500μl PBS with 0.1% Triton X-100. Lysates were kept on ice and mixed 2:1 with the following solution: 180μg/ml SDS, 1% Triton, 350μg/ml p-nitrophenyl laurate (PNL) in PBS. PNL required incubation at 65°C for 20 minutes to solubilize, and was cooled to room temperature before use. Absorbance (405nm) was measured as $Time_{30min} - Time_{0min}$.

Statistics

All statistical tests were performed by unpaired, two-tailed t-test.

Results

Mutation in the *GMP synthetase* gene causes hepatic steatosis in zebrafish

The *s850* mutant was originally identified in a large-scale mutagenesis screen focusing on liver development(20) as a mutant showing reduced liver size (Supplementary fig. 1). A positional cloning approach identified the *s850* mutation as a T to A transition in an exon of the *GMP synthetase* gene that changes the conserved histidine (H^{189}) to glutamine (Q) (Supplementary fig. 2). Subsequently, we found that in *GMP synthetase*^{s850} mutant larvae, hepatocytes start accumulating neutral lipid as indicated by whole-mount Oil Red O (ORO) staining at 7 days post fertilization (dpf) (Fig. 1A and B). Approximately 30% of *GMP synthetase*^{s850} mutant larvae showed clear ORO staining in the liver at 7dpf (Fig. 1E). In *GMP synthetase*^{s850} mutant larvae, ORO staining in the liver was also observed at 8 and 9 dpf (Fig. 1E). In order to investigate hepatic steatosis in *GMP synthetase*^{s850} mutant larvae with subcellular-resolution, we developed a method in which we stained cytoplasmic lipid droplets by fluorescent Nile Red(21) and observed their intracellular localization in three dimensions by confocal microscopy (Fig. 1C and D). This method allowed us to precisely count the portion of hepatocytes containing one or more lipid droplets. In *GMP synthetase*^{s850} mutant larvae, on average, 36.5% of hepatocytes contained Nile Red positive lipid droplets (S.D. 13.8; n=10; $p < 0.01$), while in their wild-type siblings, the percentage of hepatocytes containing Nile Red signal was significantly lower (average 5.5%; S.D. 6.7; n=9) (Fig. 1F). Consistently, when we treated *GMP synthetase*^{s850} mutant larvae with 150 μM GMP, the percentage of hepatocytes containing lipid droplets was reduced (average 13.5%; S.D. 12.7; n=9), suggesting that insufficient GMP production might induce hepatic steatosis in *GMP synthetase*^{s850} mutant larvae. Electron micrographs confirmed the existence of lipid droplets in *GMP synthetase*^{s850} mutant hepatocytes (Supplementary fig. 3). Consistent with hepatic steatosis, the total triglyceride level is increased in *GMP synthetase*^{s850} mutant larvae (Fig. 1G).

De novo GMP synthesis is required to prevent hepatic steatosis

Previous studies indicated that the proliferation of leukocytes in mammals(22) and axon guidance in the *Drosophila* visual system(23) require *de novo* GMP synthesis. However, the precise mechanisms by which *de novo* GMP synthesis regulates these biological processes are not clear. The final two steps of the *de novo* GMP synthesis pathway are linear and rate-limiting steps in which inosine monophosphate (IMP) dehydrogenase catalyzes the oxidation of IMP to xanthosine monophosphate (XMP) and GMP synthetase catalyzes the amination of XMP to GMP (Fig. 1H). In order to distinguish whether *de novo* GMP synthesis or unknown signaling or regulatory effects of GMP synthetase are responsible for hepatic steatosis, we treated wild-type zebrafish larvae with mycophenolic acid (MPA), a small molecule inhibitor of IMP dehydrogenase(24), to downregulate *de novo* GMP synthesis activity. We found that treating wild-type larvae with 15 μg/ml MPA from 3 to 7 dpf induced hepatic steatosis at 7 dpf (Fig. 1I and J), suggesting inhibition of *de novo* GMP synthesis is sufficient to induce hepatic steatosis. Consistently, we counted the number of Nile Red-positive hepatocytes in MPA-treated larvae (Average 26.2%; S.D. 10.5; n=12) and found significantly more hepatocytes containing lipid droplets (Fig. 1K-M) than in control DMSO-treated larva (average 2.1%; S.D. 1.7; n=12). Altogether, these data uncover a new role for *de novo* GMP synthesis in TG metabolism and hepatic steatosis in zebrafish.

De novo GMP synthesis is required for activation of the small GTPase Rac1

In *Drosophila, de novo* GMP synthesis is required to activate the small GTPase Rac1(23). We hypothesized that in zebrafish *GMP synthetase*^{s850} mutant larvae, the supply of GMP, and hence GTP, is compromised, leading to a decrease in the activity of small GTPases including Rac1. To test this hypothesis, we measured GTP-bound (activated) Rac1 levels using a Pak1-binding domain (PBD) pull-down assay (Fig. 2A). We found that GTP-bound Rac1 levels are decreased in *GMP synthetase*^{s850} mutant and MPA-treated larvae (Fig. 2), suggesting that de novo GMP synthesis is required for the full activation of Rac1.

Inhibition of Rac1 activity in hepatocytes induces hepatic steatosis

Interestingly, we found that inhibiting Rac1 activity is sufficient to induce hepatic steatosis (Fig. 3A and B). When treated with 50 μg/ml Rac1 inhibitor-containing media for 48 hours from 5 dpf, the activity of Rac1 was down-regulated in larvae (Fig. 2) as expected, and we found that a majority of treated larvae developed hepatic steatosis as indicated by increased Oil Red O staining in liver (Fig. 3B and C). To our knowledge, this is the first in vivo data suggesting a link between small GTPases and the regulation of hepatic steatosis. We counted the number of Nile Red-positive hepatocytes in Rac1 inhibitor-treated larvae (average 35.6%; S.D. 12.5; n=9) and found significantly more hepatocytes containing lipid droplets than in DMSO-treated control larvae (average 2.1%; S.D. 1.7; n=12) (Fig. 3E, F and H).

After observing that Rac1 is expressed strongly in hepatocytes at 7 dpf (Fig. 3D; supplementary fig. 4), we hypothesized that Rac1 activity in hepatocytes is required for the prevention of hepatic steatosis. To test this hypothesis, we generated a new transgenic line, *Tg(fabp10:GFP*-DNRac1)^{lri4}, which expresses dominant negative Rac1 (N17) only in hepatocytes (Supplementary fig. 5). In *Tg(fabp10:GFP*-DNRac1)^{lri4} larvae, the percentage of hepatocytes containing lipid droplets stained by Nile Red is significantly higher (average 32.7%; S.D. 11.9; n=12) (Fig. 3G and H; supplementary fig. 5), suggesting that Rac1 activity in hepatocytes is important for the regulation of hepatic steatosis.

Homeostatic generation of ROS is necessary to prevent hepatic steatosis

Historically, the role of Rac1 in actin cytoskeletal reorganization has been extensively studied(25); however, it is also known that Rac1 forms a protein complex with NADPH oxidases (Nox) to regulate their function in generating the superoxide anion that is quickly dismuted to hydrogen peroxide (H_2O_2) and other ROS molecules(10, 11, 26). Since accumulating evidence indicates that ROS are important components in cell signaling, we hypothesized that Rac1 regulates hepatic steatosis through Nox-mediated ROS production. To test this hypothesis, we inhibited the activity of Nox by the flavoprotein inhibitor, diphenyliodonium(10) (DPI). We found that larvae treated with 10 μM DPI from 5 dpf showed strong Oil Red O signal in the liver at 7 dpf (Fig. 4A and B). We also confirmed that the percentage of hepatocytes containing lipid droplets stained by Nile Red is significantly higher in DPI-treated larva (Average 30.8%; S.D. 12.5; n=11) (Fig. 4D and F). These data suggest that down-regulating Nox activity is sufficient to induce hepatic steatosis. To test whether Nox mediated ROS production is important for the prevention of hepatic steatosis, we treated larvae with the ROS-quenching agent *N*-acetyl cysteine(8) (NAC). We found that in larvae treated with 50 μM NAC from 5 dpf, the percentage of hepatocytes containing lipid droplets is significantly increased at 7 dpf (average 47.4%; S.D. 6.9; n=9) (Fig. 4E and F). These data suggest that a reduction in ROS production might be responsible for the induction of hepatic steatosis.

To test this hypothesis, we next measured whole-body ROS production in DPI-treated, MPA-treated, Rac1 inhibitor-treated and *GMP synthetase*^{s850} mutant larvae. As expected, in 10 μM DPI-treated larva, the production of ROS throughout the body was significantly reduced (Fig. 4G). Indeed, we found that ROS production was also reduced in MPA-treated and Rac1 inhibitor-treated and *GMP synthetase*^{s850} mutant larvae (Fig. 4G and H), supporting the hypothesis that a reduction in ROS production might be responsible for the induction of hepatic steatosis. To further test this hypothesis, we treated larvae with 1mM hydrogen peroxide (H_2O_2), which increased internal ROS levels as indicated by fluorescence of the ROS indicator, H2DCF (Fig. 4I) without any morphological changes at 7dpf, and asked if increasing ROS levels would rescue hepatic steatosis. When we treated *GMP synthetase*^{s850} mutant larvae with 1mM H_2O_2 from 4 to 7 dpf, lipid droplets in hepatocytes were significantly decreased (average 10.5%; S.D. 9.7; n=10; $p<0.05$) (Fig. 4J–L), suggesting that artificially increasing ROS ameliorated hepatic steatosis in *GMP synthetase* mutant larvae. Consistently, 1mM H_2O_2 treatment from 5 to 7 dpf, eliminated lipid droplets in hepatocytes of Rac1 inhibitor-treated larvae (average 1.8%; S.D. 2.9; n=9; $p<0.01$) (Fig. 4M), further supporting the notion that ROS homeostasis is important for the prevention of hepatic steatosis.

ROS production influences *triglyceride hydrolase* gene expression

To understand the molecular mechanisms by which ROS generation influences hepatic steatosis, we used microarray analysis to look for genes that are affected by both the *GMP synthetase* mutation and Rac1 inhibitor-treatment in a similar manner. Among the candidates satisfying this criterion, we focused on the *triglyceride hydrolase* (*tgh*) gene, which codes for an enzyme responsible for the mobilization of stored triglyceride in hepatocytes(4, 5, 7). We first verified the down-regulation of *tgh* gene expression in *GMP synthetase*^{s850} mutant and Rac1 inhibitor-treated larvae by quantitative RT-PCR (qPCR, Fig. 5A). Since down-regulation of Triglyceride hydrolase (TGH) activity is sufficient to induce lipid droplet accumulation in hepatocytes(4), we hypothesized that the Rac1 mediated ROS production regulates *tgh* gene expression to control lipid droplet formation in hepatocytes. Supporting this hypothesis, it was found that the expression level of the *tgh* gene was also reduced in DPI-treated larvae (Fig. 5A). Consistent with these gene expression changes, the enzymatic activity of TGH(6) in *GMP synthetase*^{s850} mutant, Rac1 inhibitor-treated, and

DPI-treated larvae was also reduced (Fig. 5B), suggesting that Rac1 mediated ROS production influences TGH activity by regulating its expression. The *tgh* gene is expressed only in the yolk syncytial layer (YSL) at 3 dpf (data not shown), however its expression is restricted to the liver by 5 dpf and it remains expressed only in the liver at 7dpf (Fig. 5C).

Inhibition of hydrolase activity in cultured hepatocytes by a small molecule inhibitor, Diethyl *p*-nitrophenyl phosphate (E600), was shown to attenuate mobilization of TG[7](7). Thus, we hypothesized that decreased hydrolase activity causes hepatic steatosis by attenuating the mobilization of transiently stored TG in hepatocytes. To test this hypothesis, we treated zebrafish larvae with 10 μM E600 from 5 to 7 dpf and found that the hydrolase enzymatic activity was reduced in E600-treated larvae (Fig. 5D). We further found that E600-treated larvae developed strong hepatic steatosis (Fig. 5F and H), with more than 20% of hepatocytes containing lipid droplets stained by Nile Red (Fig. 5G–I) in all E600-treated larvae examined (average 42.4%; S.D. 14.1; n=10), suggesting that the inhibition of hydrolase activity is sufficient to induce hepatic steatosis in zebrafish larvae.

Since decreased ROS production down-regulates *tgh* gene expression, we hypothesized that ROS production levels are correlated with *tgh* gene expression levels. To test this hypothesis, we treated larvae with 1mM H_2O_2 from 5 to 7 dpf and examined the expression level of *tgh* mRNA. We found that *tgh* mRNA expression was increased in the 1mM H_2O_2 -treated larvae (Fig. 5J), supporting the hypothesis that ROS levels positively regulate *tgh* gene expression. Finally, we treated *GMP synthetase*^{s850} mutant larvae, in which ROS production and *tgh* gene expression are reduced, with 1mM H_2O_2 from 5 to 7 dpf, and examined the expression level of the *tgh* mRNA. We found that *tgh* mRNA expression was restored to wild-type levels in H_2O_2-treated *GMP synthetase*^{s850} mutant larva (Fig 5J), suggesting that increasing ROS is sufficient to rescue down-regulation of *tgh* transcription in *GMP synthetase*^{s850} mutant larvae.

Discussion

In this study, we show that *de novo* GMP synthesis is necessary to prevent hepatic steatosis in zebrafish (Fig. 1). *De novo* GMP synthesis influences the activation of the small GTPase Rac1, and Rac1 promotes the production of reactive oxygen species (ROS) (Fig. 6), which is important in regulating hepatic lipid dynamics by controlling *triglyceride hydrolase* gene expression (Fig. 6). Given that down-regulating Rac1 activity, by overexpressing dominant negative Rac1 specifically in hepatocytes, was sufficient to induce hepatic steatosis (Fig. 3G and H), this signaling cascade appears to take place in hepatocytes.

Mycophenolic acid influences the production of ROS

Hydrogen peroxide (H_2O_2), a relatively stable ROS that functions as a signaling molecule, mediates communication between wounded tissues and leukocytes(27). Mycophenolic acid (MPA) is a Food and Drug Administration (FDA) approved drug that has been used for immunosuppression(24), however the precise molecular mechanisms by which MPA suppresses immune reaction are not clear. In this study, we show that in MPA-treated larvae, the production of ROS was reduced (Fig. 4F). This reduction in ROS production is most likely due to reduced activation of Rac1 (Fig. 2). Based on these results, we suggest that MPA suppresses the immune response, at least in part, by affecting Rac1 mediated ROS production.

Hepatic steatosis in *GMP synthetase* mutant larvae

We observed hepatic steatosis in *GMP synthetase*^{s850} mutant larvae (Fig. 1). Consistently, we also observed increased total triglyceride (TG) level in these animals (Fig. 1G), however,

since we measured the triglyceride level in a whole-body, this could be due to increased TG levels in extrahepatic tissues.

Although both intrahepatic biliary and vascular networks exist in *GMP synthetase*^{s850} mutant larvae at 7 dpf (Supplementary fig 6), their livers are smaller likely due to reduced cell proliferation (Supplementary fig. 1). Since liver size is not rescued in hydrogen peroxide (H_2O_2)-treated *GMP synthetase*^{s850} mutant larvae (data not shown), and Rac1 inhibitor-treated, DPI-treated, E600-treated (data not shown) and *Tg(fabp10:GFP*-DNRac1*)*^{lri4} larvae have normal liver size (Supplementary fig. 5), we conclude that the liver cell proliferation phenotype in *GMP synthetase*^{s850} mutant larvae appears to be independent of the ROS-mediated pathway.

Consistent with a previous study(28), *GMP synthetase*^{s850} mutant larvae also display smaller eyes, the absence of xanthopore pigmentation, and dysmorphic branchial arches. However, these phenotypes were not rescued by H_2O_2 treatment (data not shown), suggesting that these phenotypes are also independent of the ROS-mediated pathway.

Hepatic steatosis is a risk factor for progression to nonalcoholic steatohepatitis (NASH), which is associated with inflammation. In *GMP synthetase*^{s850} mutant larvae, inflammation is not evident at 7 dpf, as evidenced by a lack of neutrophil infiltration to the liver at this stage (Supplementary fig. 7). However, these data do not exclude the possibility of the presence of other types of immune cells in the livers of *GMP synthetase*^{s850} mutant larvae.

At 7 dpf, the percentage of *GMP synthetase*^{s850} mutant larvae showing ORO staining in the liver is relatively low (Fig. 1E). Since MPA treatment to *GMP synthetase*^{s850} mutant larvae further increased the percentage of ORO staining at 7 dpf (Supplementary fig. 8), maternally deposited *GMP synthetase* mRNA or protein might be influencing the results, or the *s850* allele might not be a null.

We did not observe any hepatic steatosis at 5 or 6 dpf in *GMP synthetase*^{s850} mutant larvae (data not shown). Similarly, Rac1 inhibitor or DPI treatment from 3 to 5 dpf did not induce hepatic steatosis in wild-type larvae (Supplementary fig. 9). The observation that the *triglyceride hydrolase* (*tgh*) gene is expressed in the liver only after 5 dpf (Fig. 5C) may explain why down-regulating ROS production does not induce hepatic steatosis before 5 dpf. Consistent with this hypothesis, Rac1 inhibitor or DPI treatment induces significant hepatic steatosis after 6 dpf both in starved and fed wild-type larvae (Supplementary Fig. 9 and 10).

Triglyceride hydrolase (tgh) gene regulation by ROS levels

We showed that expression of *tgh* is correlated with ROS levels. In *GMP synthetase*^{s850} mutant, Rac1 inhibitor-treated, and DPI-treated larvae, in which ROS production is reduced (Fig. 4G and H), relative *tgh* expression is down-regulated (Fig. 5A). Conversely, in H_2O_2-treated larvae, the expression of *tgh* was increased (Fig. 5J). Down-regulating TGH activity level by E600 (Fig. 5D) to the level in *GMP synthetase*^{s850} mutant larvae (Fig. 5B) was sufficient to induce hepatic steatosis (Fig. 5E–I), supporting the hypothesis that reduced *tgh* expression is responsible for hepatic steatosis in *GMP synthetase*^{s850} mutant larvae.

A previous study indicated that hepatic TG levels in Tgh-null mice were not statistically different from those in wild-type mice(5). In mice, Tgh also acts in white adipose tissues(5) and it is likely that the absence of hepatic steatosis in tgh-null mice is due to decreased fatty acids delivery to the liver from adipose tissue, since isolated Tgh-null hepatocytes in culture accumulate more exogenous lipids than wild-type hepatocytes(4). In contrast, zebrafish

white adipose tissues only develop after 12 dpf(29), potentially explaining why suppressing Tgh activity was sufficient to induced hepatic steatosis at 7 dpf.

In *GMP synthetase*^{s850} mutant larvae, expression of genes involved in *de novo* lipogenesis (*srebp1*, *acc1*, *agapt*, and *fads2*), β-oxidation (*aco*, *cpt1*, *cyp4a10*, and *echs1*) or lipid uptake (*cd36*) are not significantly changed at 6 dpf (Supplementary fig. 11). These data also support the hypothesis that reduced *tgh* expression is responsible for hepatic steatosis in *GMP synthetase*^{s850} mutant larvae.

Under physiological conditions, ROS produced by β-oxidation of triglyceride-derived free fatty acids may provide feedback to influence Tgh activity, adjusting lipid dynamics in hepatocytes.

ROS and hepatic steatosis

ROS are recognized to play important roles in host defense, especially in the innate immune response of leukocytes to pathogens(10), though the excessive production of ROS frequently results in inflammatory responses in many tissues, including the liver. In the liver, the two hit model has been proposed for the transition of hepatic steatosis to more severe NASH, in which the first hit is hepatic steatosis and the second hit is ROS-mediated inflammation(30). Our data provide genetic evidence that physiological ROS levels are also necessary for the prevention of hepatic steatosis in zebrafish larvae (Fig. 6). The ability of H_2O_2 to rescue hepatic steatosis in *GMP synthetase*^{s850} mutant, Rac1 inhibitor-treated, and *Tg(fabp10:*GFP-DNRac1*)*^{lri4} larvae (Fig. 4 and 6) further supports this idea. Our data do not, however, conflict with the current two hit model or the notion that excess ROS production is pathological; rather we propose that a reduction in physiological levels of ROS can be equally pathogenic to increased levels of ROS. These data suggest that proposed antioxidant supplementation for the treatment of NAFLD(31) would require careful dosage control to ensure that ROS levels are not reduced below their physiologically normal levels.

Supplementary Material

Refer to Web version on PubMed Central for supplementary material.

Acknowledgments

We thank Laura Nagy, Sanjoy Roychowdhury, Jasmine Lau, Takao Sakai, and Thomas McIntyre for critical reading of the manuscript. This work was supported in part by grants from the NIH (R00 DK078138) and CWRU/Cleveland Clinic CTSA (UL1RR024989) and a startup package from the Cleveland Clinic Foundation to T.F.S. This work was also supported by grants from the NIH (R01DK60322) and Packard foundation to D.Y.R.S.

Abbreviations

NAFLD	non-alcoholic fatty liver disease
TG	triglyceride
NASH	nonalcoholic steohepatitis
TGH	triglyceride hydrolase
ROS	reactive oxygen species
GMP	guanosine monophosphate
GDP	guanosine diphosphate
GTP	guanosine triphosphate

dpf	days post-fertilization
IMP	inosine monophosphate
XMP	xanthosine monophosphate
MPA	mycophenolic acid
PBD	Pak1-binding domain
DPI	diphenyliodonium
E600	Diethyl *p*-nitrophenyl phosphate

References

1. Cohen JC, Horton JD, Hobbs HH. Human fatty liver disease: old questions and new insights. Science. 2011; 332:1519–1523. [PubMed: 21700865]
2. Speliotes EK, Yerges-Armstrong LM, Wu J, Hernaez R, Kim LJ, Palmer CD, Gudnason V, et al. Genome-wide association analysis identifies variants associated with nonalcoholic fatty liver disease that have distinct effects on metabolic traits. PLoS Genet. 2011; 7:e1001324. [PubMed: 21423719]
3. Holmes RS, Wright MW, Laulederkind SJ, Cox LA, Hosokawa M, Imai T, Ishibashi S, et al. Recommended nomenclature for five mammalian carboxylesterase gene families: human, mouse, and rat genes and proteins. Mamm Genome. 2010; 21:427–441. [PubMed: 20931200]
4. Wang H, Wei E, Quiroga AD, Sun X, Touret N, Lehner R. Altered lipid droplet dynamics in hepatocytes lacking triacylglycerol hydrolase expression. Mol Biol Cell. 2010; 21:1991–2000. [PubMed: 20410140]
5. Wei E, Ben Ali Y, Lyon J, Wang H, Nelson R, Dolinsky VW, Dyck JR, et al. Loss of TGH/Ces3 in mice decreases blood lipids, improves glucose tolerance, and increases energy expenditure. Cell Metab. 2010; 11:183–193. [PubMed: 20197051]
6. Gilham D, Lehner R. Techniques to measure lipase and esterase activity in vitro. Methods. 2005; 36:139–147. [PubMed: 15893936]
7. Gilham D, Ho S, Rasouli M, Martres P, Vance DE, Lehner R. Inhibitors of hepatic microsomal triacylglycerol hydrolase decrease very low density lipoprotein secretion. FASEB J. 2003; 17:1685–1687. [PubMed: 12958176]
8. Rolo AP, Teodoro JS, Palmeira CM. Role of oxidative stress in the pathogenesis of nonalcoholic steatohepatitis. Free Radic Biol Med. 2012; 52:59–69. [PubMed: 22064361]
9. Finkel T. Oxygen radicals and signaling. Curr Opin Cell Biol. 1998; 10:248–253. [PubMed: 9561849]
10. Bedard K, Krause KH. The NOX family of ROS-generating NADPH oxidases: physiology and pathophysiology. Physiol Rev. 2007; 87:245–313. [PubMed: 17237347]
11. Abo A, Pick E, Hall A, Totty N, Teahan CG, Segal AW. Activation of the NADPH oxidase involves the small GTP-binding protein p21rac1. Nature. 1991; 353:668–670. [PubMed: 1922386]
12. Zalkin H, Dixon JE. De novo purine nucleotide biosynthesis. Prog Nucleic Acid Res Mol Biol. 1992; 42:259–287. [PubMed: 1574589]
13. Peveri P, Heyworth PG, Curnutte JT. Absolute requirement for GTP in activation of human neutrophil NADPH oxidase in a cell-free system: role of ATP in regenerating GTP. Proc Natl Acad Sci U S A. 1992; 89:2494–2498. [PubMed: 1312725]
14. Matthews RP, Lorent K, Manoral-Mobias R, Huang Y, Gong W, Murray IV, Blair IA, et al. TNFalpha-dependent hepatic steatosis and liver degeneration caused by mutation of zebrafish S-adenosylhomocysteine hydrolase. Development. 2009; 136:865–875. [PubMed: 19201949]
15. Cinaroglu A, Gao C, Imrie D, Sadler KC. Activating transcription factor 6 plays protective and pathological roles in steatosis due to endoplasmic reticulum stress in zebrafish. Hepatology. 2011; 54:495–508. [PubMed: 21538441]

16. Thakur PC, Stuckenholz C, Rivera MR, Davison JM, Yao JK, Amsterdam A, Sadler KC, et al. Lack of de novo phosphatidylinositol synthesis leads to endoplasmic reticulum stress and hepatic steatosis in cdipt-deficient zebrafish. Hepatology. 2011; 54:452–462. [PubMed: 21488074]

17. Hugo SE, Cruz-Garcia L, Karanth S, Anderson RM, Stainier DY, Schlegel A. A monocarboxylate transporter required for hepatocyte secretion of ketone bodies during fasting. Genes Dev. 2012; 26:282–293. [PubMed: 22302940]

18. Passeri MJ, Cinaroglu A, Gao C, Sadler KC. Hepatic steatosis in response to acute alcohol exposure in zebrafish requires sterol regulatory element binding protein activation. Hepatology. 2009; 49:443–452. [PubMed: 19127516]

19. Schaub M, Nussbaum J, Verkade H, Ober EA, Stainier DY, Sakaguchi TF. Mutation of zebrafish Snapc4 is associated with loss of the intrahepatic biliary network. Dev Biol. 2012; 363:128–137. [PubMed: 22222761]

20. Ober EA, Verkade H, Field HA, Stainier DY. Mesodermal Wnt2b signalling positively regulates liver specification. Nature. 2006; 442:688–691. [PubMed: 16799568]

21. Greenspan P, Mayer EP, Fowler SD. Nile red: a selective fluorescent stain for intracellular lipid droplets. J Cell Biol. 1985; 100:965–973. [PubMed: 3972906]

22. Gu JJ, Stegmann S, Gathy K, Murray R, Laliberte J, Ayscue L, Mitchell BS. Inhibition of T lymphocyte activation in mice heterozygous for loss of the IMPDH II gene. J Clin Invest. 2000; 106:599–606. [PubMed: 10953035]

23. Long H, Cameron S, Yu L, Rao Y. De novo GMP synthesis is required for axon guidance in Drosophila. Genetics. 2006; 172:1633–1642. [PubMed: 16322525]

24. Gummert JF, Barten MJ, Sherwood SW, van Gelder T, Morris RE. Pharmacodynamics of immunosuppression by mycophenolic acid: inhibition of both lymphocyte proliferation and activation correlates with pharmacokinetics. J Pharmacol Exp Ther. 1999; 291:1100–1112. [PubMed: 10565830]

25. Hall A. Rho GTPases and the actin cytoskeleton. Science. 1998; 279:509–514. [PubMed: 9438836]

26. Bokoch GM, Diebold BA. Current molecular models for NADPH oxidase regulation by Rac GTPase. Blood. 2002; 100:2692–2696. [PubMed: 12351373]

27. Niethammer P, Grabher C, Look AT, Mitchison TJ. A tissue-scale gradient of hydrogen peroxide mediates rapid wound detection in zebrafish. Nature. 2009; 459:996–999. [PubMed: 19494811]

28. Ng A, Uribe RA, Yieh L, Nuckels R, Gross JM. Zebrafish mutations in gart and paics identify crucial roles for de novo purine synthesis in vertebrate pigmentation and ocular development. Development. 2009; 136:2601–2611. [PubMed: 19570845]

29. Imrie D, Sadler KC. White adipose tissue development in zebrafish is regulated by both developmental time and fish size. Dev Dyn. 2010; 239:3013–3023. [PubMed: 20925116]

30. Mehta K, Van Thiel DH, Shah N, Mobarhan S. Nonalcoholic fatty liver disease: pathogenesis and the role of antioxidants. Nutr Rev. 2002; 60:289–293. [PubMed: 12296456]

31. Lieber CS. S-Adenosyl-L-methionine and alcoholic liver disease in animal models: implications for early intervention in human beings. Alcohol. 2002; 27:173–177. [PubMed: 12163146]

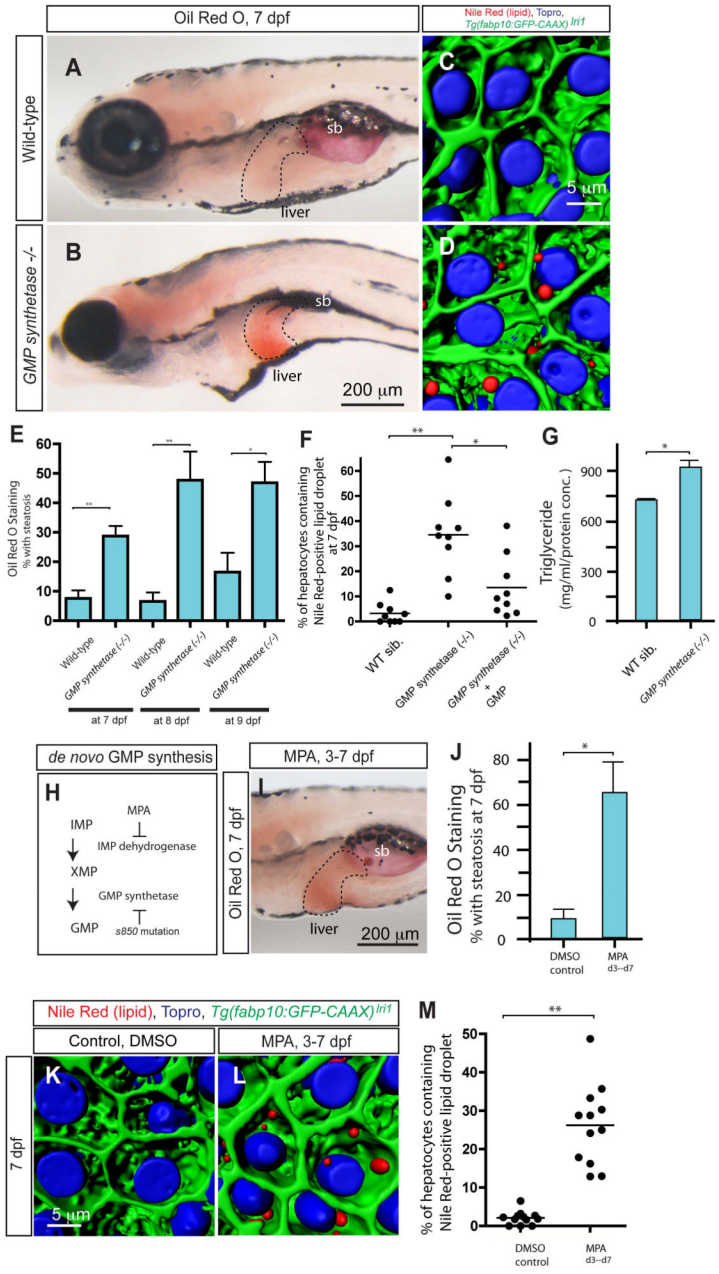

Figure 1.

Lack of *de novo* GMP synthesis leads to hepatic steatosis. (A and B) Lateral views of wild-type sibling and *GMP synthetase*^{s850} mutant larvae stained with Oil Red O (ORO) at 7 days post fertilization (dpf). *GMP synthetase*^{s850} mutant larvae develop liver steatosis at 7 dpf. Broken lines outline the liver. (C and D) Projected confocal images of the wild-type sibling (C) and *GMP synthetase*^{s850} mutant (D) liver visualized for Nile Red (red) and To-pro-3 (blue) staining and *Tg(fabp10:GFP-CAAX)*^{lri1} (green) expression at 7 dpf. In *GMP synthetase*^{s850} mutant larvae, lipid droplets stained by Nile Red are evident in hepatocytes. (E) The percentage of wild-type and *GMP synthetase*^{s850} mutant larvae showing liver steatosis scored by whole-mount ORO staining at 7, 8 and 9 dpf. ORO staining experiments with wild-type larvae at 7, 8 and 9 dpf were repeated five times (total n = 138 larvae examined and total n = 4 showed ORO signal in the liver), five times (total n = 74 larvae

examined and total n = 9 showed ORO signal in the liver) and six times (total n = 67 larvae examined and total n = 13 showed ORO signal in the liver), respectively. ORO staining experiments with *GMP synthetase*^{s850} mutant larvae at 7, 8 and 9 dpf were repeated five times (total n = 124 larvae examined and total n = 36 showed ORO signal in the liver), four times (total n = 34 larvae examined and total n = 15 showed ORO signal in the liver) and three times (total n = 26 larvae examined and total n = 12 showed ORO signal in the liver), respectively. (F) Quantification of liver steatosis measured by the percentage of hepatocytes containing Nile Red positive lipid droplets in wild-type sibling (n = 9), *GMP synthetase*^{s850} mutant (n = 9) and 150μM GMP treated *GMP synthetase*^{s850} mutant larvae (n = 9). The percentage of hepatocytes containing lipid droplets is significantly increased in *GMP synthetase*^{s850} mutant larvae. (G) Triglyceride levels measured in whole-body extracts of wild-type and *GMP synthetase*^{s850} mutant larvae at 7 dpf. (H) A schematic of the *de novo* GMP synthesis pathway. In the linear *de novo* GMP synthesis pathway, IMP is converted to XMP by IMP dehydrogenase, and subsequently, XMP is converted to GMP by GMP synthetase. Mycophenolic acid (MPA) inhibits the function of IMP dehydrogenase. The *s850* mutation disrupts the function of GMP synthetase. (I) Wild-type larvae exposed to MPA from 3 to 7 dpf were fixed and stained with ORO at 7 dpf. MPA-treated larvae developed liver steatosis. (J) The percentage of control DMSO or MPA-treated larvae showing liver steatosis scored by whole-mount ORO staining at 7dpf. MPA treatment increased the percentage of larvae showing liver steatosis. ORO staining experiments with MPA-treated larvae were repeated three times with an average n = 35.4 larvae per experiment (total n = 106 larvae examined and total n = 70 larvae showed ORO signal in the liver). (K and L) Projected confocal images of wild-type larvae treated with DMSO (K) or MPA (L) from 3 to 7 dpf visualized for Nile Red (Red) and To-pro-3 (Blue) staining and *Tg(fabp10:GFP-CAAX)*^{lri1} expression (green). Nile Red stains lipid droplets, and Topro stains nuclei. (M) Quantification of liver steatosis measured by the percentage of hepatocytes containing lipid droplets in DMSO-treated control and MPA-treated larvae at 7 dpf. MPA-treatment significantly increased the percentage of hepatocytes containing lipid droplets. sb, swim bladder. *P<0.05, **P<0.01; error bars indicate standard deviation.

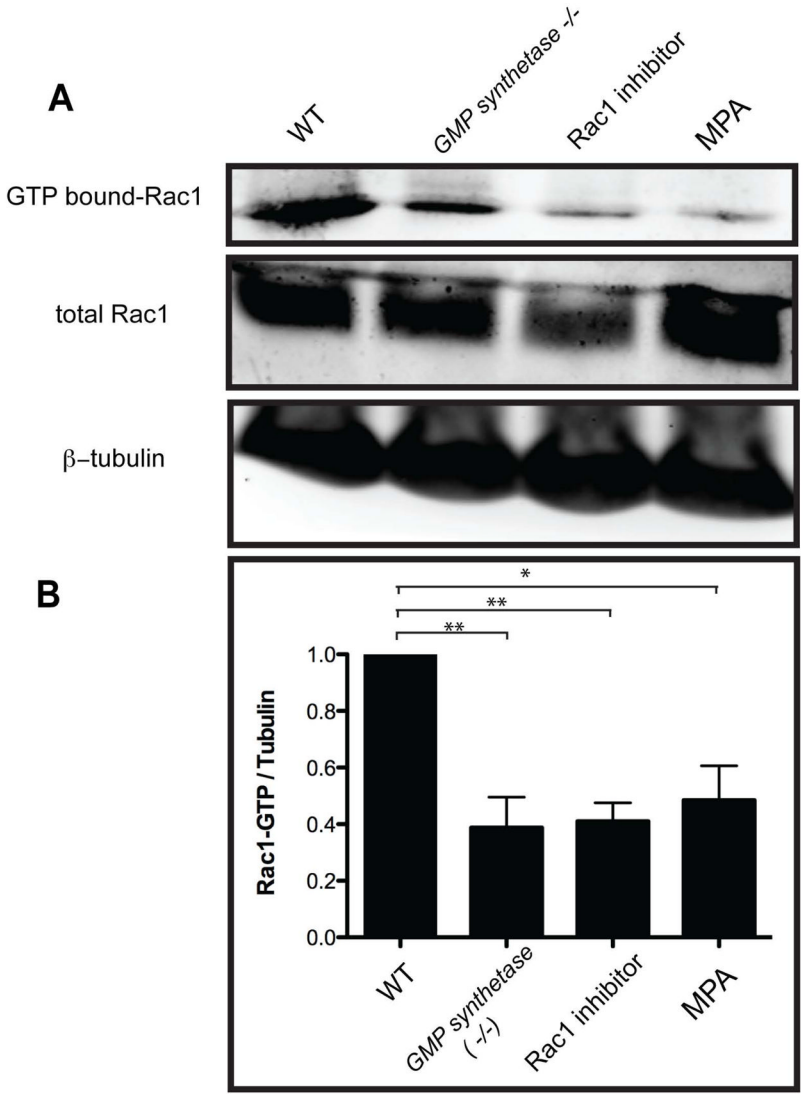

Figure 2.

De novo GMP synthesis is required for the activation of Rac1. (A) Guanosine 5′-triphosphate (GTP)-bound Rac1 levels in wild-type, *GMP synthetase*^{s850} mutant, Rac1 inhibitor treated and MPA treated larvae at 7 dpf were measured by using the PBD pull-down assay. (B) Densitometric analysis of GTP-bound Rac1 levels from three independent experiments. GTP-bound Rac1 levels were determined by using the PBD pull-down assay and normalized to β-tubulin levels. All tested conditions showed significant down-regulation of activated Rac1. *P<0.05, **P<0.01; error bars indicate standard deviation.

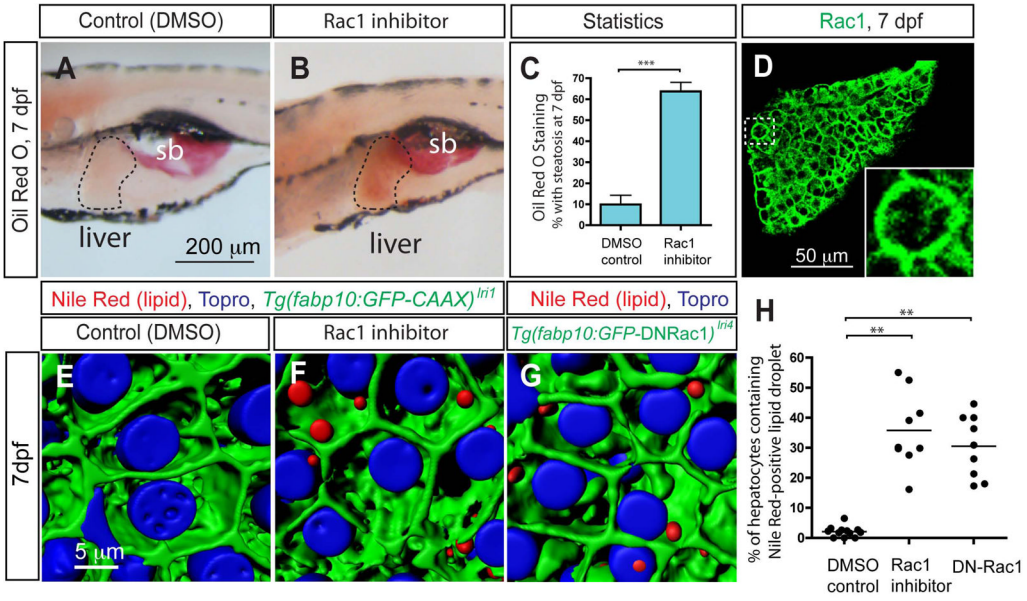

Figure 3.

The small GTPase Rac1 regulates hepatic steatosis. (A and B) Lateral views of wild-type larvae treated with DMSO (A) or Rac1 inhibitor (B) from 5 to 7 dpf and stained for ORO at 7 dpf. Rac1 inhibitor-treated larvae developed hepatic steatosis. (C) The percentage of DMSO or Rac1 inhibitor-treated larvae showing liver steatosis scored by whole-mount ORO staining. ORO staining experiments with Rac1 inhibitor-treated larvae were repeated twelve times with an average n = 12.1 larvae per experiment (total n = 146 larvae examined and total n = 89 larvae showed ORO signal in the liver). (D) Z-plane confocal image of the dissected liver of wild-type larvae visualized for Rac1 expression at 7 dpf. Rac1 is localized to the entire cell membrane of most cells in the liver. The outlined area is magnified and shown in bottom right corner. (E and F) Projected confocal images of lipid droplets in the liver stained by Nile Red. *Tg(fabp10:GFP-CAAX)*^{lri1} larvae treated with DMSO (E) or Rac1 inhibitor (F) visualized for GFP expression and Nile Red (Red) and To-pro-3 (Blue) staining at 7dpf. (G) Projected confocal image of *Tg(fabp10:GFP*-DNRac1*)*^{lri4} liver visualized for GFP expression and Nile Red (Red) and To-pro-3 (Blue) staining at 7dpf. (H) Quantification of liver steatosis measured by the percentage of hepatocytes containing Nile Red positive lipid droplets in DMSO-treated control, Rac1 inhibitor-treated and *Tg(fabp10:GFP*-DNRac1*)*^{lri4} larvae at 7 dpf. *P<0.05, **P<0.01, ***P<0.001; error bars indicate standard deviation.

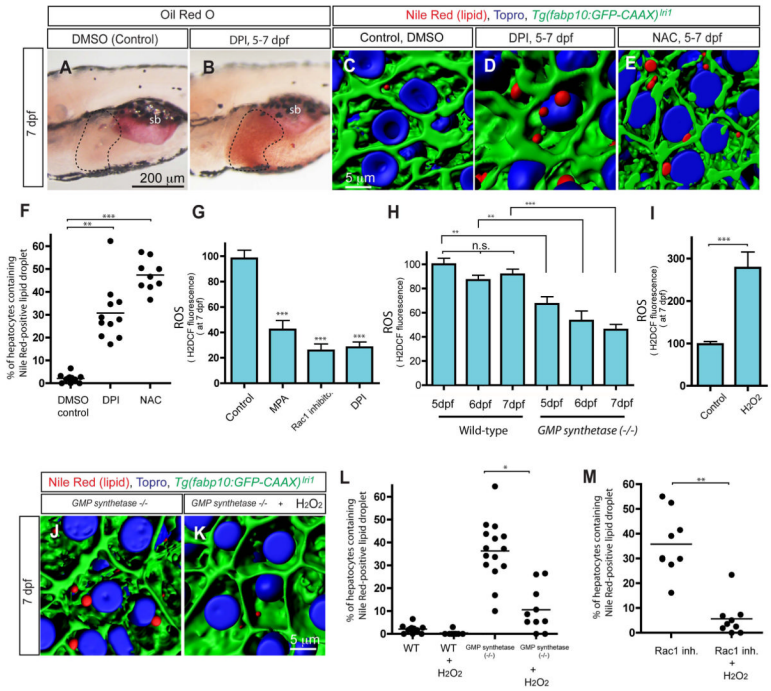

Figure 4.

Reactive Oxygen Species (ROS) homeostasis is necessary for the prevention of hepatic steatosis. (A and B) Lateral views of wild-type larvae treated with DMSO (A) or diphenyleneiodonium chloride (DPI) (B) from 5 to 7 dpf and stained for ORO at 7 dpf. Flavoprotein inhibitor, DPI, treated larvae (average 67.2%; s.d. 12.6; $p<0.001$) developed hepatic steatosis. ORO staining experiments with DPI-treated larvae were repeated five times with an average n = 12.2 larvae per experiment (total n = 61 larvae examined and total n = 41 larvae showed ORO signal in the liver). (C–E) Projected confocal images of lipid droplets in the liver stained by Nile Red. *Tg(fabp10:GFP-CAAX)*^{lri1} larvae treated with DMSO (C), DPI (D) or *N*-acetyl cysteine (NAC) (E) visualized for GFP expression and Nile Red (Red) and To-pro-3 (Blue) staining at 7dpf. (F) Quantification of liver steatosis measured by the percentage of Nile Red positive lipid droplets containing hepatocytes in DMSO, DPI or NAC treated larvae at 7 dpf. (G–I) Measurement of whole-body ROS production by H_2DCF fluorescence. Arbitrary units of H_2DCF fluorescence from three different experiments (n > 50) were normalized to control and averaged. Production of ROS in control, MPA-treated, Rac1 inhibitor-treated, and DPI-treated larvae was measured at 7 dpf (G). All tested conditions showed significant reduction of ROS production in (G). Production of ROS in wild-type and *GMP synthetase*^{s850} mutant larvae was measured at 5, 6 and 7 dpf (H). In wild-type larvae, the ROS production levels between 5 and 7 dpf were not significantly changed, while in *GMP synthetase*^{s850} mutant larvae, the ROS production level at 7dpf was reduced compared to that at 5 dpf (H). Production of ROS in control and hydrogen peroxide-treated larvae was measured at 7 dpf (I). (J and K) Hepatic steatosis in *GMP synthetase*^{s850} mutant larvae was ameliorated by hydrogen peroxide treatment. Projected confocal images of lipid droplets in the liver stained by Nile Red. *GMP synthetase*^{s850} mutant larvae cultured in the absence (J) or presence (K) of 1mM hydrogen peroxide were visualized for for Nile Red (red) and To-pro-3 (blue) staining and *Tg(fabp10:GFP-CAAX)*^{lri1} expression (green) at 7 dpf. Nile Red positive lipid droplets in the liver are reduced in hydrogen peroxide-treated *GMP synthetase*^{s850} mutant larvae. (L) Quantification of liver steatosis measured by the percentage of hepatocytes containing Nile Red positive lipid droplet in wild-type, hydrogen peroxide-treated wild-type, *GMP*

synthetase^{s850} mutant and hydrogen peroxide-treated *GMP synthetase*^{s850} mutant larvae at 7 dpf. Hydrogen peroxide treatment ameliorated hepatic steatosis in *GMP synthetase*^{s850} mutant larvae. (M) Quantification of liver steatosis measured by the percentage of hepatocytes containing Nile Red positive lipid droplets in Rac1 inhibitor-treated and Rac1 inhibitor plus hydrogen peroxide-treated larvae at 7dpf. Hydrogen peroxide treatment suppressed Rac1 inhibitor induced hepatic steatosis. n.s., not significant; *P<0.05, **P<0.01, ***P<0.001; error bars indicate standard deviation.

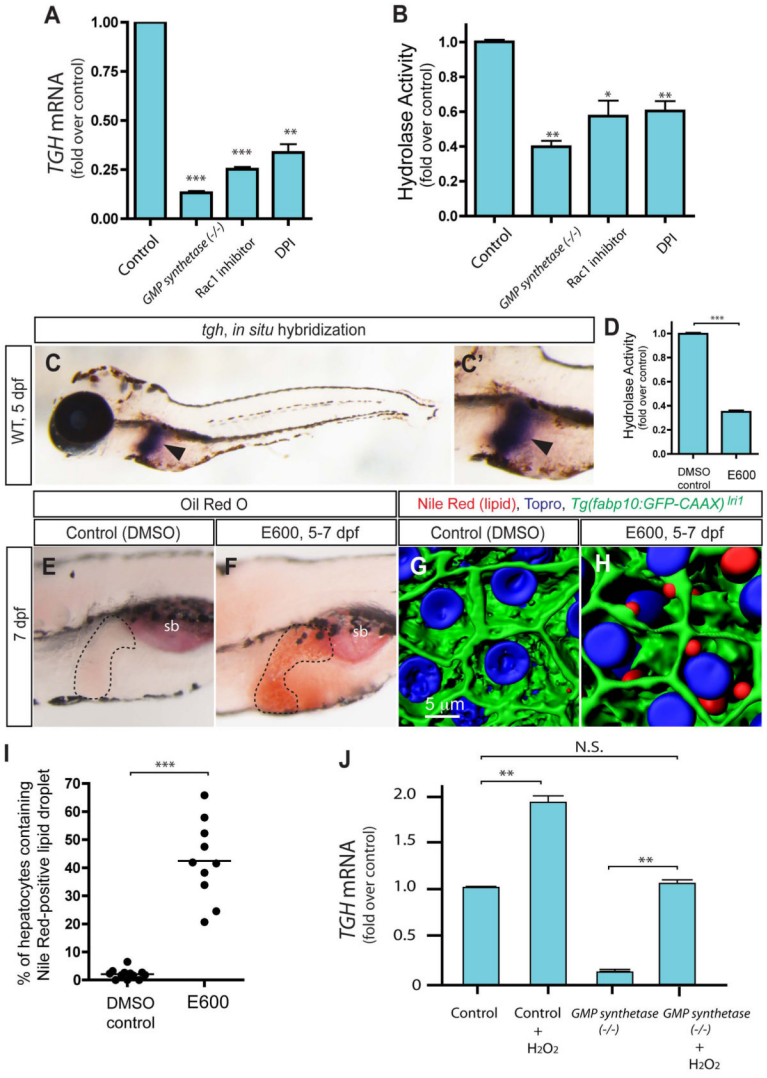

Figure 5.

Expression of *the triglyceride hydrolase* (*tgh*) gene is regulated by Rac1 mediated ROS. (A) qPCR analysis of *tgh* mRNA expression levels in wild-type control, *GMP synthetase*^{s850} mutant, Rac1 inhibitor-treated and DPI-treated larvae at 7 dpf. The averages of at least three independent experiments are shown. *tgh* mRNA expression level is significantly down-regulated in all tested conditions. (B) Hydrolysis activity toward p-nitrophenyl laurate was measured using lysates of control, *GMP synthetase*^{s850} mutant, Rac1 inhibitor-treated and DPI-treated larvae at 7 dpf. Measured activity was normalized to control and the average of three different experiments is shown. Hydrolysis activities are significantly decreased in all tested cases. (C) *tgh* expression in 5 dpf wild-type larvae. Lateral views, anterior to the left. The region around the liver is magnified and shown separately in C′. The expression of *tgh* is restricted to the liver at this stage. Arrowheads point to the liver. (D) The hydrolysis activity of the homogenate of 7dpf larvae is measured in the absence or presence of Dimethyl-p-nitrophenyl phosphate (E600). E600 significantly down-reregulated hydrolysis activity. (E and F) Lateral views of DMSO- (C) or E600- (D) treated larvae stained for ORO at 7 dpf. Hydrolase inhibitor, E600, treated larvae (Average 62.2%; s.d. 10.6; $p<0.001$) developed hepatic steatosis. The black broken lines outline the liver. ORO staining experiments with E600-treated larvae were repeated six times with an average n = 14 larvae

per experiment (total n = 84 larvae examined and total n = 52 larvae showed ORO signal in the liver). (G and H) Projected confocal images of lipid droplets in the liver stained by Nile Red. *Tg(fabp10:GFP-CAAX)*^{lri1} larvae treated with DMSO (G) or E600 (H) visualized for GFP expression and Nile Red (Red) and To-pro-3 (Blue) staining at 7dpf. (I) Quantification of liver steatosis measured by the percentage of hepatocytes containing Nile Red positive lipid droplets in DMSO- or E600-treated larvae at 7 dpf. E600-treated larvae developed hepatic steatosis. (J) qPCR analysis of *tgh* mRNA expression levels in wild-type, hydrogen peroxide-treated wild-type, *GMP synthetase*^{s850} mutant and hydrogen peroxide-treated *GMP synthetase*^{s850} mutant larvae. *tgh* mRNA expression levels were restored to the level of wild-type control in hydrogen peroxide treated *GMP synthetase*^{s850} mutant larvae. *P<0.05, **P<0.01, ***P<0.001, n.s., not significant; error bars indicate standard deviation.

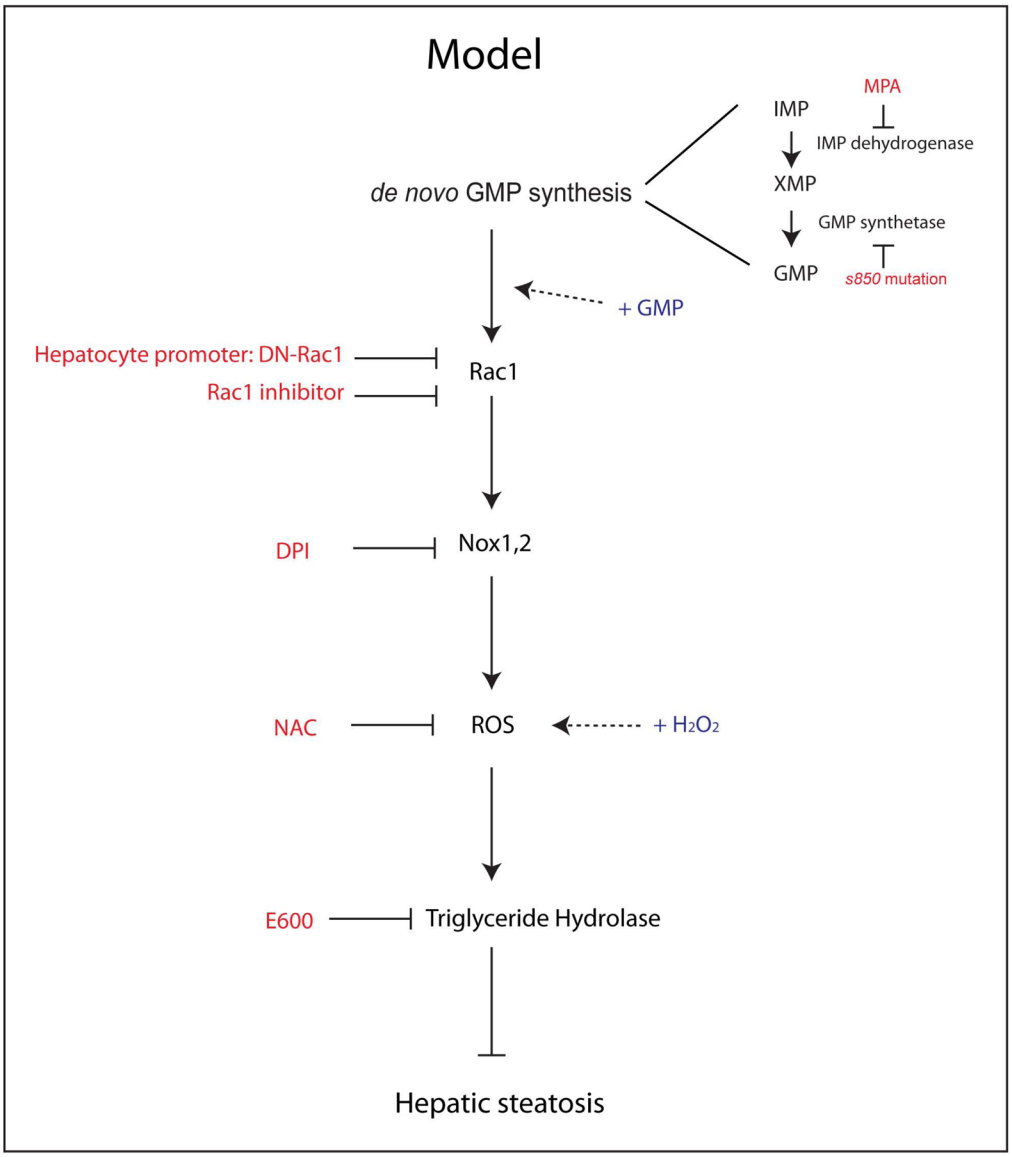

Figure 6.

Schematic model of ROS mediated liver protection from hepatic steatosis. Inhibiting *de novo* GMP synthesis by MPA-treatment or the *GMP synthetase*^{s850} mutation induced hepatic steatosis. Supplying GMP rescued the hepatic steatosis phenotype in *GMP synthetase*^{s850} mutant larva. *De novo* GMP synthesis influenced the activation of Rac1 and inhibiting Rac1 activity in hepatocytes by overexpressing dominant negative Rac1 (DN-Rac1) also induced hepatic steatosis. Rac1 regulates the activity of NADPH oxidases (Nox1, 2) and inhibiting NADPH oxidases mediated ROS production by DPI or quenching ROS by *N*-acetyl cysteine (NAC) also induced hepatic steatosis. Supplying hydrogen peroxide (H_2O_2) rescued the hepatic steatosis phenotype in *GMP synthetase*^{s850} mutant, Rac1 inhibitor-treated, and DN-Rac1 expressing larvae. ROS levels influenced *triglyceride hydrolase* gene expression. The small molecule inhibitor for Triglyceride hydrolase (E600) treatment also induced hepatic steatosis.